Activation of Phosphatidylinositol-3′-kinase/AKT Signaling Is Essential in Hepatoblastoma Survival

Wolfgang Hartmann,[1,2] Jan Küchler,[2] Arend Koch,[2,4] Nicolaus Friedrichs,[1] Anke Waha,[2] Elmar Endl,[3] Jacqueline Czerwitzki,[1] Dagmar Metzger,[1] Susanne Steiner,[1] Peter Wurst,[3] Ivo Leuschner,[5] Dietrich von Schweinitz,[6] Reinhard Buettner,[1] and Torsten Pietsch[2]

Abstract

Purpose: Hepatoblastoma represents the most frequent malignant liver tumor in childhood. The phosphatidylinositol-3′-kinase (PI3K)/AKT pathway is crucial in downstream signaling of multiple receptor tyrosine kinases of pathogenic importance in hepatoblastoma. Increased PI3K/AKT signaling pathway activity and activating mutations of *PIK3CA*, encoding a PI3K catalytic subunit, have been reported in different childhood tumors. The current study was done to analyze the role of PI3K/AKT signaling in hepatoblastoma.

Experimental Design: Immunohistochemical stainings of (Ser473)-phosphorylated (p)-AKT protein, its targets p-(Ser9)-GSK-3β and p-(Ser2448)-mTOR, as well as the cell cycle regulators Cyclin D1, $p27^{KIP1}$, and $p21^{CIP1}$ were done and the *PIK3CA* gene was screened for mutations. *In vitro*, two hepatoblastoma cell lines treated with the PI3K inhibitor LY294002 were analyzed for AKT and GSK-3β phosphorylation, cell proliferation, and apoptosis. Additionally, simultaneous treatments of hepatoblastoma with LY294002 and cytotoxic drugs were carried out.

Results: Most tumors strongly expressed p-AKT, p-GSK-3β, and p-mTOR; subgroups showed significant Cyclin D1, $p27^{KIP1}$, and $p21^{CIP1}$ expression. One hepatoblastoma carried an E545A mutation in the *PIK3CA* gene. *In vitro*, PI3K inhibition diminished hepatoblastoma cell growth being accompanied by reduced AKT and GSK-3β phosphorylation. Flow cytometry and 4′, 6-diamidino-2-phenylindole stainings showed that PI3K pathway inhibition leads to a substantial increase in apoptosis and a decrease in cellular proliferation linked to reduced Cyclin D1 and increased $p27^{KIP1}$ levels. Simultaneous treatment of hepatoblastoma cell lines with LY294002 and cytotoxic drugs resulted in positive interactions.

Conclusions: Our findings imply that PI3K signaling plays an essential role in growth control of hepatoblastoma and might be successfully targeted in multimodal therapeutic strategies.

With an annual incidence of 1.2 cases per 1 million children in western countries, hepatoblastoma is the most frequent primary malignant liver tumor in childhood (1). Although most cases of hepatoblastoma are sporadic, an increased incidence has been found in patients with familial adenomatous polyposis coli and Beckwith-Wiedemann syndrome. As in patients with Beckwith-Wiedemann syndrome, chromosomal region 11p15.5 and the insulin-like growth factor 2 gene (*IGF2*) have been shown to be frequently involved in the pathogenesis of hepatoblastoma (2–4). *IGF2* codes for an essential fetal growth factor (IGF-II), which transduces its proliferative and antiapoptotic effects preferentially through the IGF-I receptor (IGF-IR). IGF-IR is a receptor tyrosine kinase that transmits its signal via the phosphatidylinositol-3-kinase (PI3K)/AKT and the mitogen activated kinase pathways. Upon growth factor stimulation, PI3K catalyzes the generation of phosphatidylinositol-3,4,5-triphosphate (PIP_3) from phosphatidyl-inositol-4,5-triphosphate (PIP_2). PIP_3 acts as second messenger to recruit AKT/PKB, a 57-kDa Ser/Thr-kinase, to the plasma membrane where it is activated by phosphorylation through 3-phosphoinositol–dependent protein kinases. Subsequently, AKT/PKB itself phosphorylates diverse growth-controlling effectors, such as MDM2, mTOR, or GSK-3β, and (e.g. via GSK-3β or mTOR) regulates synthesis, stability, or subcellular localization of the cell cycle regulators Cyclin D1, $p21^{CIP1}$, and $p27^{KIP1}$ (5–10). D-type cyclins act as growth factor sensors and their activity is essential for the progression through the G_1 phase of the cell cycle. In contrast, the cyclin-dependent kinase (CDK) inhibitors $p21^{CIP1}$ and $p27^{KIP1}$ block CDK activity and thereby prevent the transition

Authors' Affiliations: Departments of [1]Pathology, [2]Neuropathology, and [3]Molecular Medicine and Experimental Immunology, University of Bonn Medical Center, Bonn, Germany; [4]Department of Neuropathology, Charité Universitätsmedizin, Berlin, Germany; [5]Department of Pathology, University of Kiel, Campus Kiel, Kiel, Germany; and [6]Department of Pediatric Surgery, University of Munich, Munich, Germany
Received 11/12/08; revised 4/9/09; accepted 4/17/09; published OnlineFirst 7/7/09.
Grant support: Aventis Foundation, the BONFOR program of the Medical Faculty, University of Bonn, and grant HBFG-109-517 to the Flow Cytometry Core Facility at the Institute of Molecular Medicine and Experimental Immunology, University of Bonn.
The costs of publication of this article were defrayed in part by the payment of page charges. This article must therefore be hereby marked *advertisement* in accordance with 18 U.S.C. Section 1734 solely to indicate this fact.
Note: Supplementary data for this article are available at Clinical Cancer Research Online (http://clincancerres.aacrjournals.org/).
W. Hartmann and J. Küchler contributed equally.
Requests for reprints: Wolfgang Hartmann & Torsten Pietsch, Departments of Pathology and Neuropathology, University of Bonn Medical Center, Sigmund-Freud-St. 25, D-53105 Bonn, Germany. Phone: 49-228-2871-9248; Fax: 49-228-2871-5030; E-mail: wolfgang.hartmann@uni-bonn.de, t.pietsch@uni-bonn.de.

doi:10.1158/1078-0432.CCR-08-2878

Translational Relevance

Substantial knowledge exists on the pathogenesis of hepatoblastoma, the most frequent malignant liver tumor in childhood exists, however, its therapy is still exclusively based on surgery and conventional chemotherapy only. Based on the known activation of several receptor tyrosine kinase signaling pathways in hepatoblastoma, including insulin-like growth factor signaling, we analyzed the role of the phosphatidylinositol 3′-kinase/AKT axis with respect to tumor biology and potential therapeutic applicability. Our study provides basic insights into the molecular biology of hepatoblastoma and translates them into preclinical therapeutic concepts *in vitro*.

from G_1 to S phase (11, 12). In tumors, PI3K signaling may gain independence from upstream signaling pathways by genetic alterations in different components of the pathway. Particularly, oncogenic mutations affecting the *PI3KCA* gene, which encodes the p110α phosphatidylinositol-3′-kinase catalytic subunit, have been described in colorectal cancer and embryonal tumors (13, 14).

The present study was carried out to determine if PI3K/AKT activation and mutations in the *PI3KCA* gene occur in hepatoblastoma, if PI3K/AKT activation is essential for the proliferation and survival of hepatoblastoma cells, and if targeting this pathway might be of therapeutic value.

Materials and Methods

Patients, tumors, and cell lines. A total of 47 hepatoblastoma specimens and the cell lines HUH6 (15) and HepT1 (16) were included in the mutational analysis of the *PI3KCA* gene. The patients were all enrolled in the German Society of Paediatric Haematology & Oncology (GPOH) multicenter treatment study for hepatoblastoma. The age of the patients varied from 2 to 57 mo. Constitutional genomic DNA was available in a subgroup of cases from peripheral blood for comparison. Paraffin-embedded tissue obtained at prechemotherapeutic biopsy was available from 24 patients.

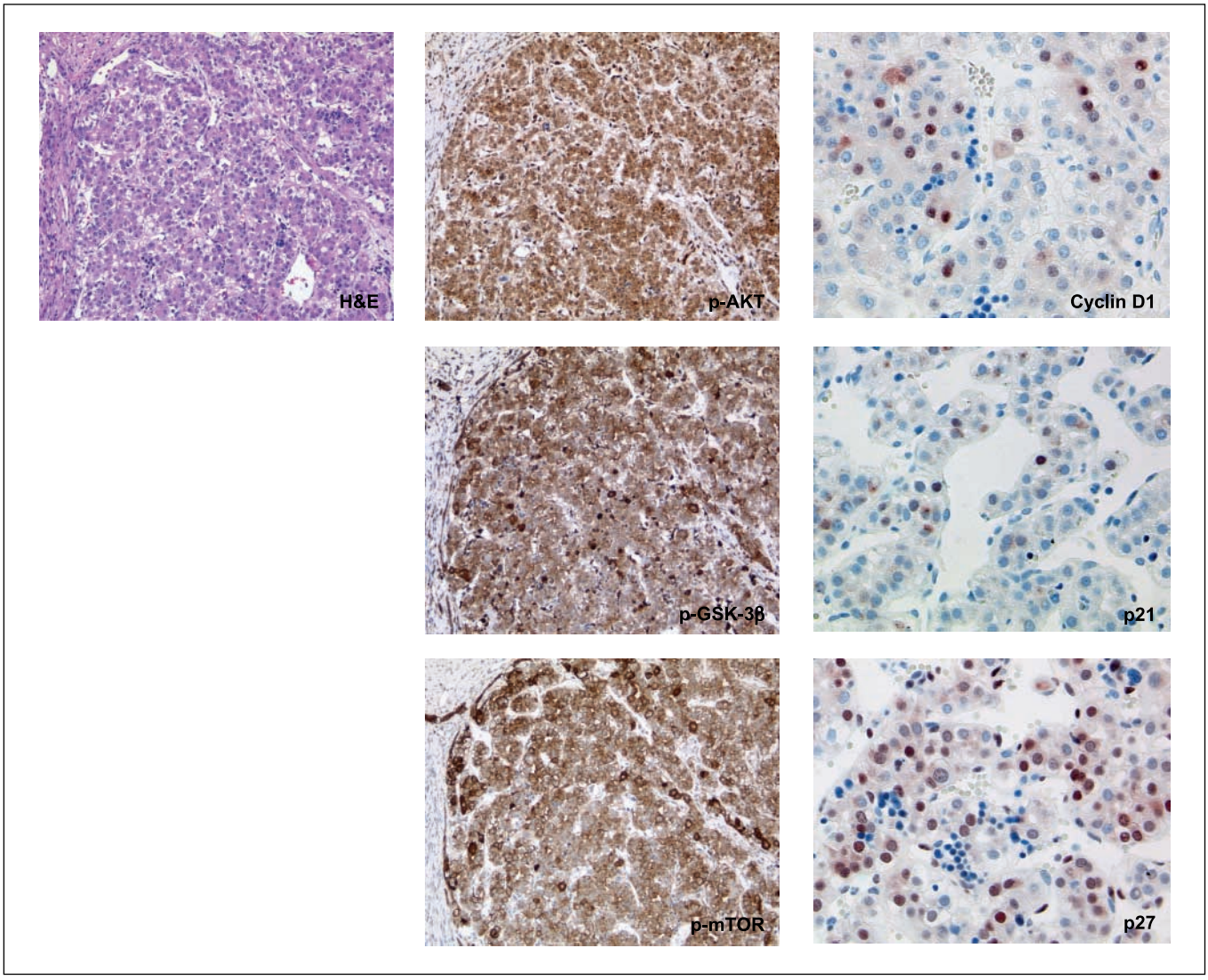

Fig. 1. Immunohistochemical analysis of p-(Ser473)-AKT, p-(Ser9)-GSK-3β, and p-(Ser2448)-mTOR (original magnification, ×100), and Cyclin D1, $p21^{CIP1}$, and $p27^{KIP1}$ (original magnification, ×200) in a representative case of hepatoblastoma.

DNA extraction. DNA was isolated from tumor tissue by a standard proteinase K/SDS digestion followed by phenol/chloroform extraction. Tissue fragments selected for DNA extraction were checked by frozen-sectioning to ensure that they consisted of tumor tissue. Only fragments with a tumor cell content of at least 80% were included.

Single-strand conformational polymorphism analysis of the* PI3KCA *gene and DNA sequencing. Mutational analysis of the *PI3KCA* gene was done in 47 hepatoblastomas and the hepatoblastoma-derived cell lines HUH6 and HepT1. Primer sequences and detailed PCR conditions are listed in Supplementary Table S1 online. All PCRs were run in a UNO Thermoblock cycler (Biometra). PCR fragments covered the coding sequence of the previously described mutational hot spot regions (exon 1, exon 9, and exon 20) of the *PIK3CA* gene. PCR was carried out in a final volume of 10 μL containing 10 to 50 ng of DNA, 5 pmol of each primer, 10 mmol/L Tris-HCl (pH 8.3), 50 mmol/L KCl, 1.0-1.5 mmol/L $MgCl_2$, 200 mmol/L of each deoxynucleotide, and 0.25 unit of *Taq* polymerase (Life Technologies). Mutational screening by single-strand conformation polymorphism (SSCP) method was done as described before (4). For detailed information on SSCP conditions, see Supplementary Table S1 online. PCR products showing aberrantly migrating bands were purified using the QIAquick PCR purification Kit (Qiagen). Sequencing was done by Entelechon GmbH.

Immunohistochemistry. For immunostainings of cultured hepatoblastoma, cells were pelleted, fixed in 3.7% buffered paraformaldehyde, and embedded in paraffin after standard dehydration. Tissue specimens were fixed in 4% buffered formaldehyde and embedded in paraffin. After antigen retrieval (10 mmol/L sodium citrate buffer, pH 6.0, microwave 600 W, 10 min) immunohistochemical stainings were done on 4-μm sections with an Autostainer (DAKO; Cyclin D1, $p21^{CIP1}$, $p27^{KIP1}$) or manually [p-(Ser473)-AKT, p-(Ser9)-GSK-3β, and p-(Ser2448)-mTOR]. For Cyclin D1, $p21^{CIP1}$, and $p27^{KIP1}$, the antigen-antibody binding was visualized by means of the avidin-biotin complex (ABC-method) using

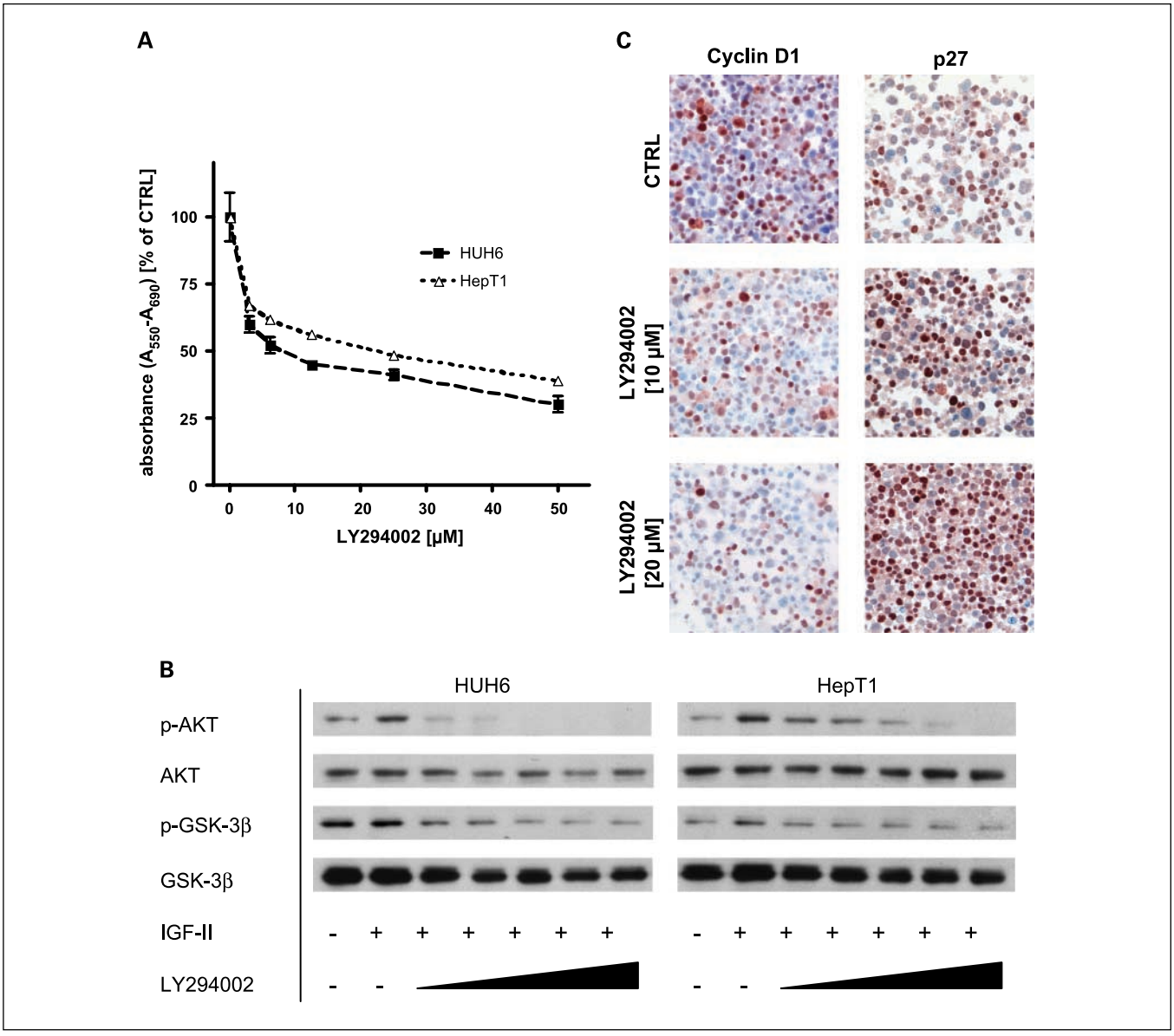

Fig. 2. *A,* MTT assay in two hepatoblastoma cell lines treated with the PI3K-inhibitor LY294002. *B,* Western blot analysis of p-(Ser473)-AKT, p(Ser9)-GSK-3β, AKT, and GSK-3β in hepatoblastoma cell lines treated with IGF-II and increasing concentrations of LY294002 (3, 6, 12, 25, and 50 μmol/L). *C,* Cyclin D1 and $p27^{KIP1}$ immunocytochemical staining of HepT1 cells treated with different doses of LY294002 for 24 h.

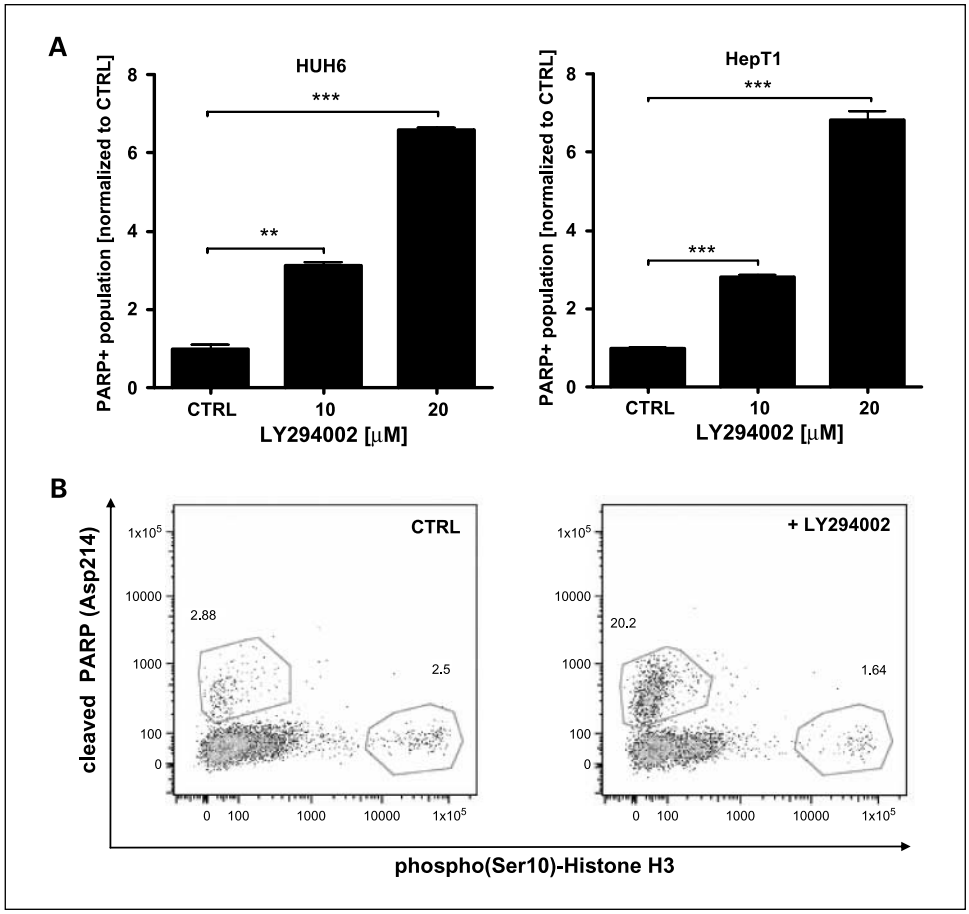

Fig. 3. *A,* results of the flow cytometric analysis: induction of apoptosis as measured by detection of cleaved PARP. *t*-test: ***, $P < 0.001$; **, $P < 0.01$. *B,* representative results of the flow cytometric analysis of phospho (Ser10) – histone H3 and cleaved PARP (Asp214) in HepT1 treated with 20 μmol/L LY294002.

AEC (3-amino-9-ethylcarbazol) as chromogen. For p-AKT, p-GSK-3β, and p-mTOR stainings, the Catalyzed Signal Amplification System (CSA II; DAKO) was employed according to the manufacturer's instructions using 3,3′-diaminobenzidine as chromogen. p-AKT, p-GSK-3β, and p-mTOR antibodies (Cell Signaling Technology) were used at a dilution of 1:100, $p27^{KIP1}$ (Abcam) at a dilution of 1:50, and $p21^{CIP1}$ (Zytomed) and Cyclin D1 (DCS) at a dilution of 1:25. Positive controls and negative control stainings employing appropriate mouse IgG (DAKO) and rabbit IgG isotypes (DCS) were included.

Culture and treatment of hepatoblastoma cells, MTT cell proliferation assay. HepT1 and HUH6 hepatoblastoma cell lines were cultured in RPMI 1640 supplemented with 10% fetal bovine serum (FBS; Invitrogen), and maintained at 37°C in a humidified 5% CO_2 atmosphere. Treatments were done with different amounts of LY294002 (Cell Signaling Technology) or DMSO as control. DMSO concentrations were <0.1%. For MTT proliferation assays, cells were cultured in 96-well dishes (Nunc) in a volume of 100 μL and a concentration of 5×10^4 cells/mL. Assays were done for 72 h, using a minimum of five replicates. For coincubation with conventional chemotherapeutic drugs, cells were treated with varying concentrations of doxorubicin (0.1-1,000 ng/mL) and cisplatin (0.1-1,000 ng/mL) with a constant dose of LY294002 (HepT1, 7.5 μmol/L; HUH6, 5 μmol/L), corresponding to a dose resulting in ~20% to 40% growth inhibition in these cell lines. Proliferation assays were done using the MTT cell proliferation kit (Roche) according to the manufacturer's instructions. The formazan dye was quantified using a scanning multiwell spectrophotometer. For flow cytometry and 4′, 6-diamidino-2-phenylindole (DAPI) stainings, cells were cultured as described above in 25-cm^2 cell culture flasks (Greiner) with a preincubation of 18 h and treatment for 24 h with 10 μmol/L and 20 μmol/L LY294002 or an appropriate control. For immunocytochemical analysis of hepatoblastoma cells, cells were treated for 24 h, harvested, pelleted, fixed in 3.7% buffered paraformaldehyde, and embedded in paraffin after standard dehydration.

Knockdown of PI3K by RNA interference. Hepatoblastoma cells were cultured in 25-cm^2 flasks in a volume of 4 mL RPMI 1640 containing 10% FBS. At a density of 30%, cells were transfected with 12 pmol (HUH6) or 40 pmol (HepT1) PIK3CA Stealth RNA (PIK3CAHSS10800 4-6, Invitrogen) or nontargeting control small interfering RNA (siRNA; Invitrogen) using Lipofectamine RNAiMAX (Invitrogen) according to the instructions of the manufacturer. After 24 h, cells were trypsinized, reseeded as described above, and MTT assays were done essentially as described above in RPMI 1640 supplemented with 2% FBS. To document p110α knockdown, 5×10^4 transfected cells were plated in 12-well dishes in medium supplemented with 2% FBS and cultured for 72 h. Protein extraction and Western blotting were done as described below using antibodies against p110α (Cell Signaling Technology) and β-actin (clone AC-15; Sigma) as internal control.

Flow cytometry. For flow cytometric immunophenotyping, 1×10^6 cells were fixed on ice in ice-cold 2% paraformaldehyde for 10 min. They were then washed in PBS, collected by centrifugation, resuspended and incubated in ice-cold PBS with 0.25% Triton X-100 for 5 min on ice. After another washing step, cells were resuspended in 100 μL PBS/0.5% bovine serum albumin containing an Alexa Fluor 647-labeled phospho-(Ser10)-Histone H3 antibody (Cell Signaling Technology; 1:20) and a phycoerythrin-labeled cleaved-Poly(ADP-ribose)-polymerase (PARP; Asp214) antibody (BD Biosciences; 1:5) and incubated for 30 min at room temperature. After a further washing step, 500 μL PBS containing 10 μg/mL DAPI (Sigma) were added to stain DNA, and cells were incubated for an additional 30 min at room temperature. Analysis was done using a three-laser LSRII analytical flow cytometer (BD Biosciences). Data were analyzed using Flowjo (Tree Star) analysis software. At least 30,000 events were

recorded per experiment. Only single cells were included in the analysis. Each experiment was carried out at least in duplicate.

Cell transfection and expression vectors. The constitutively active myristoylated AKT construct (myr-AKT) and its control empty vector (pUSE) were obtained from Upstate. HepT1 cells were cultured in 25-cm^2 flasks (Greiner) in a volume of 4 mL RPMI 1640 containing 10% FBS. At a density of 50%, cells were transfected with 1.25 μg of the myr-AKT or the pUSE control plasmid together with 1.25 μg of the pmaxGFP vector (Amaxa). After 24 h, cells were trypsinized and seeded in 75-cm^2 flasks (Greiner). After another 24 h, 7.5 μmol/L LY294002 or DMSO as control were added for 24 h. Analysis was done by flow cytometry essentially as described above, including only transfected, strongly GFP-fluorescence positive cells in the analysis.

Analysis of apoptosis by DAPI staining. Cells were treated as described above. They were harvested and washed in PBS, fixed in 3.7% paraformaldehyde for 10 min at room temperature, and washed again. After incubation with 1 μg/mL DAPI (Sigma) for 10 min and two further washing steps cells were mounted on appropriate slides using Fluoromount-G medium (Southern Biotechnologies Associates, Inc.). Nuclei were visualized and photographed using a Leica DMLB fluorescence microscope. Apoptotic cells were morphologically defined by chromatin condensation and fragmentation. For each assay at least 300 cells were analyzed in triplicate.

Western blot analysis. Cells were cultured as described above in 12-well dishes (Nunc) in a volume of 1 mL for 18 h before treatment. Four hours prior to treatments, cells were washed twice with TBS and medium was replaced by serum-free Neurobasal medium (Invitrogen). Different doses of LY294002 were added immediately after the application of 200 ng/mL recombinant human IGF-II. Incubation was done for 5 min. Cell lysis and Western blots were done as described before (17). Filters were incubated with p-(Ser473)-AKT, p-(Ser9)-GSK3β, AKT, and GSK3β (Cell Signaling Technology) antibodies according to the instructions of the manufacturer. Secondary antibody labeling as well as filter development were done using the ECL kit (Amersham) as described before.

Results

Hepatoblastomas exhibit significant expression of p-(Ser473)-AKT, p-(Ser9)-GSK-3β, and p-(Ser2448)-mTOR. Immunohistochemistry revealed strong p-AKT expression in 79% (19 of 24) of the cases; 5 cases showed moderate p-AKT levels. p-GSK-3β was strongly expressed in 75% (18/24) of the cases; 6 cases had a focal staining pattern. Two of the latter cases simultaneously displayed lower p-AKT expression. p-mTOR was strongly expressed in 96% (23/24 cases); the case with lower expression concomitantly showed lower p-GSK-3β but strong p-AKT expression. Significant Cyclin D1 protein expression was detectable in 35% of the cases (7/20), all of them simultaneously displaying strong p-AKT expression; 13 cases displayed foci of weakly stained cells. Thirty-nine percent (9/23) of the tumors exhibited significant p27^{KIP1} expression; in 61% (14/23) of the cases, single cells or small groups of cells were stained. All significantly p27^{KIP1}-positive tumors belonged to the group strongly expressing p-AKT. There was an overlap of four cases in the Cyclin D1- and p27^{KIP1}-expressing subgroups. Finally, p21^{CIP1} was detectable in 38% (9/24) of the tumors, most of them displaying a focal and weak staining result; no correlation with p-AKT, p-GSK-3β, or p-mTOR expression was discernible (Fig. 1).

PI3K pathway activation may rarely be due to **PI3KCA** *mutations in hepatoblastoma.* A total of 47 hepatoblastoma samples and the two hepatoblastoma cell lines HUH6 and HepT1 were included in a mutational analysis of the previously described hot spot regions of the *PI3KCA* gene. One case (D773), showing an aberrant pattern in SSCP, was found to carry the known activating point-mutation E545A (GAG→GCG) in exon

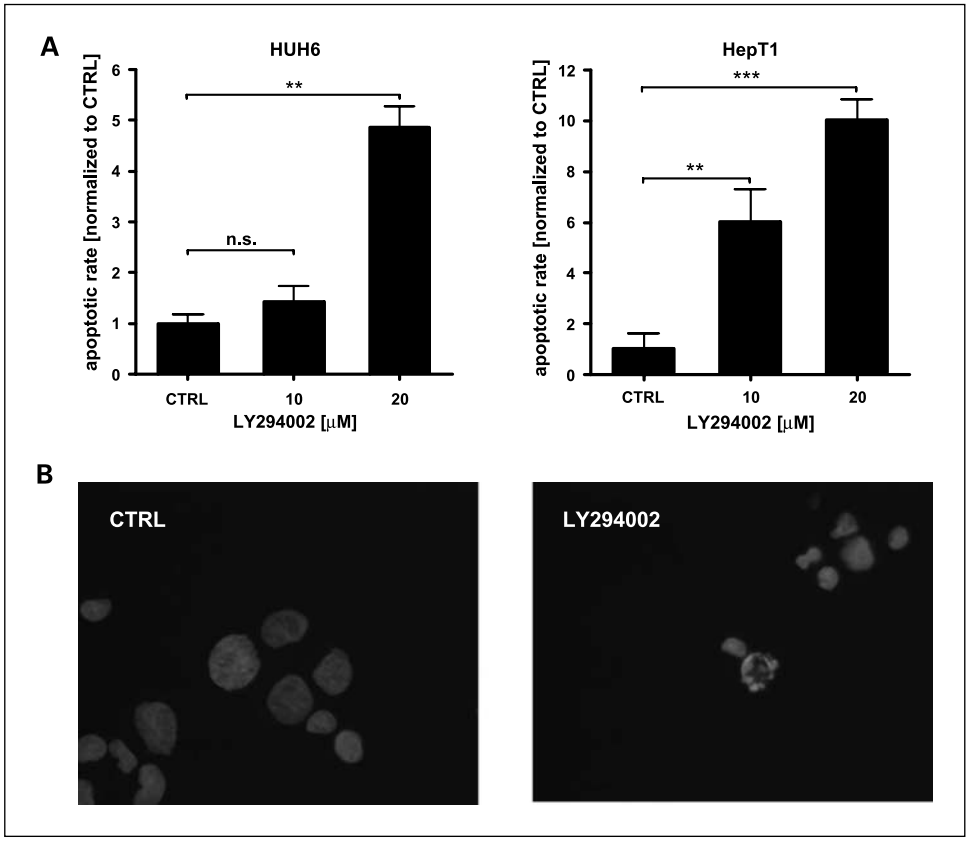

Fig. 4. *A,* apoptotic rate of LY294002-treated hepatoblastoma cells as measured by DAPI stainings; *t*-test: ***, $P < 0.001$; **, $P < 0.01$; n.s., not significant. *B*, representative DAPI-staining results of HUH6 cells treated with 10 μmol/L LY294002.

9 (18, 19). This mutation is localized in the helical domain of PI3K and results in a gain of kinase activity (20).

Growth of human hepatoblastoma cells depends on an activated PI3K/AKT signaling pathway. The hepatoblastoma cell lines HUH6 and HepT1 were cultured with increasing concentrations of the PI3K inhibitor LY294002. Both cell lines showed a dose-dependent growth inhibition in MTT assays. The 50% growth inhibition (GI_{50}) levels were calculated using Prism Version 4.0a for Macintosh. GI_{50} was 8 μmol/L for HUH6 and 20 μmol/L for HepT1 (Fig. 2A).

PI3K signaling inhibition in hepatoblastoma cell lines is associated with reduced phosphorylation of AKT and GSK-3β. In order to elucidate the role of downstream signaling pathways affected by PI3K, IGF-II–stimulated hepatoblastoma cells were treated with different concentrations of LY294002 (3-50 μmol/L) and tested for phosphorylation of AKT (Ser473) and GSK-3β (Ser9). In both cell lines a dose-dependent reduction of AKT and GSK-3β phosphorylation was documented (Fig. 2B). Immunocytochemical stainings of HepT1 cells treated with different doses of LY294002 for 24 hours revealed a dose-dependent reduction of nuclear Cyclin D1 and an increase of nuclear $p27^{KIP1}$ protein levels (Fig. 2C) whereas the levels of $p21^{CIP1}$ and p-(Ser2448)-mTOR did not show a significant change (data not shown).

Induction of apoptosis is the major but not sole mechanism of LY294002-dependent growth reduction. In order to analyze if the effect of LY294002 on hepatoblastoma cells was predominantly proapoptotic or antimitotic, we did a flow cytometric analysis of cleaved PARP (Asp214) as an indicator of apoptosis and phospho-(Ser10)-Histone H3, a marker of mitosis. In both cell lines, LY294002-induced growth reduction was significantly associated with an increase of the cell population positive for cleaved PARP (t-test, $P < 0.001$; Fig. 3A and B). HepT1 cells additionally showed a significant decrease of the phospho-(Ser10)-Histone H3–positive subpopulation (10 μmol/L: 69% of control, t-test, $P < 0.01$; 20 μmol/L: 61% of control, t-test, $P < 0.01$) whereas mitotic activity was not significantly affected in HUH6 (data not shown). Correspondingly, microscopic analysis of DAPI-stained cells showed a significant increase of nuclei displaying chromatin fragmentation or condensation in both cell lines (Fig. 4A and B).

RNA interference–mediated PI3KCA knockdown mimics, constitutive AKT activation counteracts LY294002-effected PI3K inhibition in hepatoblastoma. To provide additional evidence for the relevance of PI3K/AKT signaling in hepatoblastoma cells, and to indirectly document specificity of the effect seen with LY294002, we additionally transfected both hepatoblastoma cell lines with PI3KCA siRNAs. Cell growth as measured by MTT assays was reduced to 43.9 ± 0.60% in HUH6 and to 52.9 ± 0.44% in HepT1 cells compared with the mock-transfected control, and strong down-regulation of p110α protein could be documented in Western blots (Fig. 5A).

To find out if an activated AKT signal is able to counteract the inhibitory effects of LY294002, we overexpressed myr-AKT in HepT1 cells. In the control experiment using the empty pUSE vector, treatment with 7.5 μmol/L LY294002 (corresponding to the dose used in the combination experiments with conventional chemotherapeutic drugs) led to a decrease of the mitotic phospho(Ser10)-Histone H3–positive fraction to 40 ± 2% (t-test, $P < 0.01$), whereas the mitotic rate was not significantly decreased in the myr-AKT–expressing population (Fig. 5B). The basic apoptotic rate in myr-AKT–expressing HepT1 cells was 43 ± 6.5% of the pUSE-transfected control cells. However, under the experimental conditions selected (employing a dose <50% of the GI_{50}), the apoptotic rate in LY294002-treated cells did not show a significant increase, either in pUSE control or myr-AKT cells (data not shown).

Inhibition of PI3K signaling sensitizes hepatoblastoma cells for chemotherapeutic treatment. HUH6 and HepT1 hepatoblastoma cells were coincubated with increasing doses of cisplatin and doxorubicin, chemotherapeutic drugs used in current chemotherapeutic protocols in the treatment of hepatoblastoma, and doses of the PI3K inhibitor LY294002 leading to 20% to 40% growth reduction. Substantial additional effects of PI3K inhibition and chemotherapeutic drugs were observed (Fig. 6).

Discussion

Activation of the PI3K/AKT signaling pathway has been described in different tumors including embryonal tumors, e.g. rhabdomyosarcoma and medulloblastoma (21, 22). Mostly, activation of the pathway occurs via enhanced growth factor

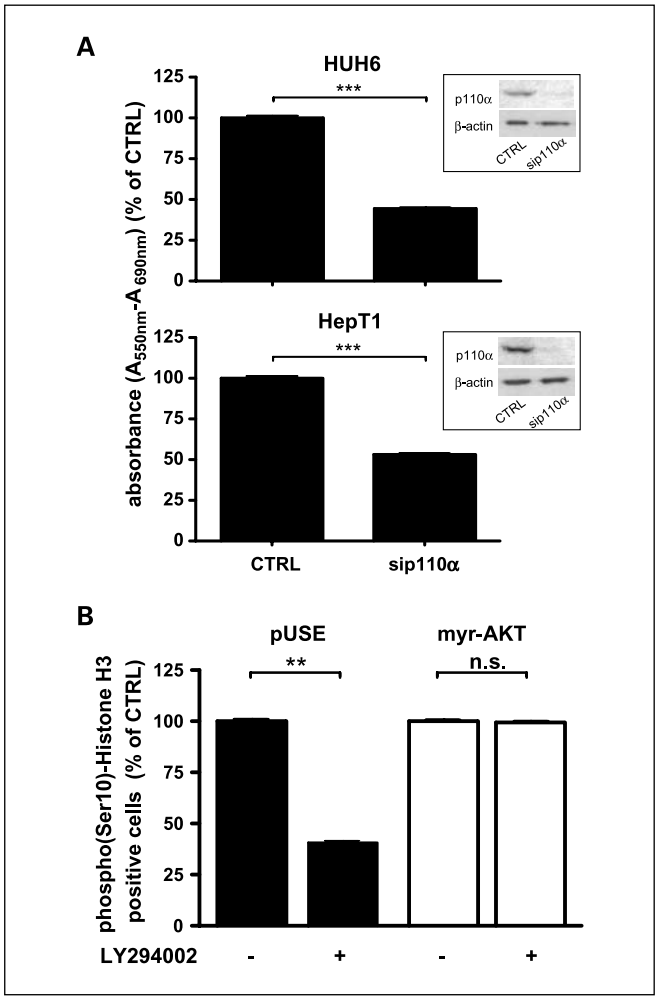

Fig. 5. *A*, siRNA-mediated knockdown of the PI3K p110α subunit (*insets*) is accompanied by a significant decrease of cell growth in HUH6 (*top*) and HepT1 (*bottom*); t-test: ***, $P < 0.001$. *B*, compensation of the antimitogenic effect of a reduced dose of LY294002 by overexpression of consitutively active myristoylated AKT in HepT1 cells; t-test: **, $P < 0.01$.

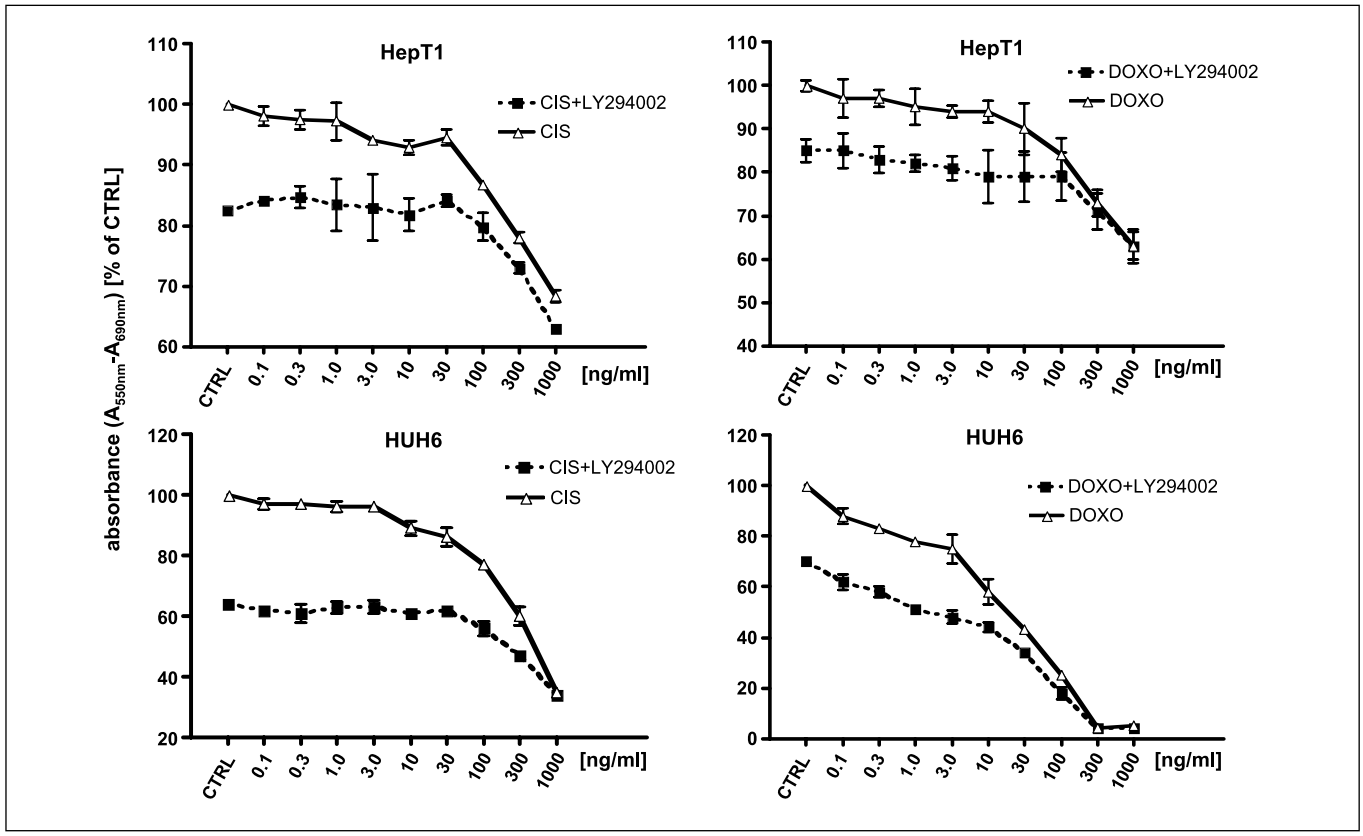

Fig. 6. Combination treatments of hepatoblastoma cells with cisplatin (CIS) and doxorubicin (DOXO) and LY294002 (HepT1, 7.5 μmol/L; HUH6, 5 μmol/L).

receptor–mediated signaling. One of the most frequent alterations described in hepatoblastoma, which is partly due to loss of imprinting in the chromosomal region 11p15.5, is drastically increased *IGF2* mRNA and protein levels (3, 4). IGF-II is a potent ligand of the IGF-I receptor tyrosine kinase, which transduces its signal mainly via the PI3K/AKT signaling pathway (23). Recently, constitutive activation of PI3K/AKT in hepatoblastoma has been described as a result of up-regulation of IGF-II (24). However, activating mutations in *PIK3CA*, encoding the p110α phosphatidylinositol 3′-kinase catalytic subunit, which have been reported for other tumors, have not been described in hepatoblastoma so far (13, 25).

To get an insight into the activation status of the PI3K signaling pathway in hepatoblastoma, we did immunohistochemical stainings of activated PI3K-downstream targets, i.e. AKT, mTOR, and GSK-3β, as well as the cell cycle regulators Cyclin D1, $p27^{KIP1}$, and $p21^{CIP1}$. mTOR is involved in cellular growth and proliferation by the control of translation of essential cellular regulator proteins including Cyclin D1 and $p27^{KIP1}$ (9, 26). On the other hand, the degradation of Cyclin D1, $p27^{KIP1}$, and $p21^{CIP1}$ is dependent on GSK-3β, which, itself, is subject to an inhibitory phosphorylation step by AKT (5, 8, 11, 27). GSK-3β is of particular interest in hepatoblastoma as it represents one of the molecular links to the *Wnt* signaling pathway, which has been reported to be of high relevance in the pathogenesis of this tumor (28, 29). GSK-3β belongs to the multiprotein complex involved in degradation of β-catenin and therefore accounts for an essential growth regulator in hepatoblastoma, particularly those cases lacking mutations of *Wnt* signaling pathway components (30).

Our immunohistochemical data document strong expression of phosphorylated AKT, GSK-3β, and mTOR in the vast majority of hepatoblastoma, indicating an activation of the pathway. The presence of subsets of tumors with significant Cyclin D1 or relatively low $p27^{KIP1}$ and $p21^{CIP1}$ expression levels implied that therapeutic targeting of PI3K/AKT signaling might be successful through interference with the cyclin/CDK inhibitor network – aiming at a shift in the balance of proproliferative and antiproliferative signals.

In the light of recent reports on activating mutations of the *PIK3CA* gene in different types of cancer, we wanted to find out if *PIK3CA* gene mutations might be responsible for the activation seen. We therefore screened a panel of 47 hepatoblastoma samples and the hepatoblastoma cell lines HUH6 and HepT1 for mutations in the hot spot regions (exons 1, 9, and 20) of the *PI3KCA* gene (13). In one hepatoblastoma sample, we detected the described E545A mutation in exon 9, which has been reported in other malignancies before (18, 19). The functional impact of this mutation in terms of an increased oncogenic potential by an increased enzymatic activity has been described before (20).

In order to get an insight into the biological relevance of PI3K/AKT signaling in hepatoblastoma, we carried out *in vitro* experiments targeting PI3K enzymatic activity. In both HUH6 and HepT1 hepatoblastoma cell lines, a significant and dose-dependent inhibition of cellular growth was observed upon treatment with LY294002 (Fig. 2A). This effect was reproducible in independent

experiments employing siRNA-mediated knockdown of the PI3K p110α subunit, indirectly implying specificity of the pharmacologic effect seen (Fig. 5A). Concomitant dose-dependent decreases in phosphorylation of AKT and, to a lesser extent, GSK-3β, further documented specific mechanisms in LY294002-mediated PI3K inhibition on the protein level (Fig. 2B).

We wanted to know if it was cellular proliferation or cell death that caused decreased signals in MTT assays. Flow cytometric analysis of cleaved PARP as a marker of apoptosis revealed a substantial dose-dependent increase of apoptotic cell death due to treatments with LY294002 in both hepatoblastoma cell lines; corresponding observations were made in the morphologic analysis of DAPI-stained nuclei in both cell lines. HepT1 cells additionally displayed a concomitant decrease of the mitotic p-(Ser10)-histone H3–positive cell fraction, which was accompanied by decreased levels of Cyclin D1 and increased nuclear levels of $p27^{KIP1}$ as detected by immunocytochemistry (Fig. 2C). The antimitogenic impact of a reduced dose of LY294002 in HepT1 was completely reversible by overexpression of constitutively activated AKT, representing a further indicator of specificity of the pharmacologic effect of LY294002 (Fig. 5B).

The changes seen in Cyclin D1 and $p27^{KIP1}$ protein levels certainly contribute to the growth-reducing and antimitogenic effect of PI3K inhibition, but as discernible from the flow cytometric data, the common trait in both hepatoblastoma cell lines is the induction of apoptosis. There are several possible pathways linking PI3K/AKT signaling to antiapoptosis, e.g. AKT promotes cell survival by phosphorylating the proapoptotic protein Bcl-2-Antagonist of Cell Death, thereby preventing its inhibitory binding to Bcl-2 (31), and GSK-3β regulates protein turnover of downstream targets including MCL1, a member of the Bcl-2 family (32).

We finally wanted to get an insight into a possible role of PI3K inhibition in the treatment of hepatoblastoma. PI3K inhibitors have been shown to increase the efficacy of conventional chemotherapeutic drugs in other tumor cells (33). To elucidate a potential therapeutic role of PI3K inhibition in future multimodal treatments of hepatoblastoma, we coincubated conventional cytotoxic drugs currently used in hepatoblastoma therapy with LY294002 and observed additive effects on cellular proliferation. This finding points to the option to employ PI3K inhibitors in multimodal therapeutic approaches, thereby minimizing the toxicity of the individual compounds.

In summary, our data show that PI3K/AKT signaling is commonly activated in hepatoblastoma and that this is due to activating mutations in the *PIK3CA* gene in a small subset of hepatoblastoma. Targeting PI3K *in vitro* results in increased apoptosis and inhibition of cellular proliferation of hepatoblastoma cells. Coincubations with conventional chemotherapeutic drugs seem promising. These findings argue in favor of PI3K as a potential therapeutic target in hepatoblastoma.

Disclosure of Potential Conflicts of Interest

No potential conflicts of interest were disclosed.

References

1. Stiller CA, Pritchard J, Steliarova-Foucher E. Liver cancer in European children: incidence and survival, 1978–1997. Report from the Automated Childhood Cancer Information System project. Eur J Cancer 2006;42:2115–23.
2. Albrecht S, von Schweinitz D, Waha A, Kraus JA, von Deimling A, Pietsch T. Loss of maternal alleles on chromosome arm 11p in hepatoblastoma. Cancer Res 1994;54:5041–4.
3. Li X, Adam G, Cui H, Sandstedt B, Ohlsson R, Ekstrom TJ. Expression, promoter usage and parental imprinting status of insulin-like growth factor II (IGF2) in human hepatoblastoma: uncoupling of IGF2 and H19 imprinting. Oncogene 1995;11:221–9.
4. Hartmann W, Waha A, Koch A, et al. p57(KIP2) is not mutated in hepatoblastoma but shows increased transcriptional activity in a comparative analysis of the three imprinted genes p57(KIP2), IGF2, and H19. Am J Pathol 2000;157:1393–403.
5. Cross DA, Alessi DR, Cohen P, Andjelkovich M, Hemmings BA. Inhibition of glycogen synthase kinase-3 by insulin mediated by protein kinase B. Nature 1995;378:785–9.
6. Vivanco I, Sawyers CL. The phosphatidylinositol 3-kinase AKT pathway in human cancer. Nat Rev Cancer 2002;2:489–501.
7. Osaki M, Oshimura M, Ito H. PI3K-Akt pathway: its functions and alterations in human cancer. Apoptosis 2004;9:667–76.
8. Diehl JA, Cheng M, Roussel MF, Sherr CJ. Glycogen synthase kinase-3β regulates cyclin D1 proteolysis and subcellular localization. Genes Dev 1998;12:3499–511.
9. Bjornsti MA, Houghton PJ. The TOR pathway: a target for cancer therapy. Nat Rev Cancer 2004;4:335–48.
10. G-Amlak M, Uddin S, Mahmud D, et al. Regulation of myeloma cell growth through Akt/Gsk3/forkhead signaling pathway. Biochem Biophys Res Commun 2002;297:760–4.
11. Liang J, Slingerland JM. Multiple roles of the PI3K/PKB (Akt) pathway in cell cycle progression. Cell Cycle 2003;2:339–45.
12. Sherr CJ. Cancer cell cycles. Science 1996;274:1672–7.
13. Samuels Y, Wang Z, Bardelli A, et al. High frequency of mutations of the PIK3CA gene in human cancers. Science 2004;304:554.
14. Broderick DK, Di C, Parrett TJ, et al. Mutations of PIK3CA in anaplastic oligodendrogliomas, high-grade astrocytomas, and medulloblastomas. Cancer Res 2004;64:5048–50.
15. Doi L. Establishment of a cell line and its clonal sublines from a patient with hepatoblastoma. Gann 1976;67:1–10.
16. Pietsch T, Fonatsch C, Albrecht S, Maschek H, Wolf HK, von Schweinitz D. Characterization of the continuous cell line HepT1 derived from a human hepatoblastoma. Lab Invest 1996;74:809–18.
17. Hartmann W, Koch A, Brune H, et al. Insulin-like growth factor II is involved in the proliferation control of medulloblastoma and its cerebellar precursor cells. Am J Pathol 2005;166:1153–62.
18. Baohua Y, Xiaoyan Z, Tiecheng Z, Tao Q, Daren S. Mutations of the PIK3CA gene in diffuse large B cell lymphoma. Diagn Mol Pathol 2008;17:159–65.
19. Kang S, Seo SS, Chang HJ, Yoo CW, Park SY, Dong SM. Mutual exclusiveness between PIK3CA and KRAS mutations in endometrial carcinoma. Int J Gynecol Cancer 2008;18:1339–43.
20. Kang S, Bader AG, Vogt PK. Phosphatidylinositol 3-kinase mutations identified in human cancer are oncogenic. Proc Natl Acad Sci U S A 2005;102:802–7.
21. Zhang J, Hu S, Schofield DE, Sorensen PH, Triche TJ. Selective usage of D-Type cyclins by Ewing's tumors and rhabdomyosarcomas. Cancer Res 2004;64:6026–34.
22. Hartmann W, Digon-Sontgerath B, Koch A, et al. Phosphatidylinositol 3′-kinase/AKT signaling is activated in medulloblastoma cell proliferation and is associated with reduced expression of PTEN. Clin Cancer Res 2006;12:3019–27.
23. Toretsky JA, Helman LJ. Involvement of IGF-II in human cancer. J Endocrinol 1996;149:367–72.
24. Tomizawa M, Saisho H. Signaling pathway of insulin-like growth factor-II as a target of molecular therapy for hepatoblastoma. World J Gastroenterol 2006;12:6531–5.
25. Bader AG, Kang S, Zhao L, Vogt PK. Oncogenic PI3K deregulates transcription and translation. Nat Rev Cancer 2005;5:921–9.
26. Hashemolhosseini S, Nagamine Y, Morley SJ, Desrivieres S, Mercep L, Ferrari S. Rapamycin inhibition of the G_1 to S transition is mediated by effects on cyclin D1 mRNA and protein stability. J Biol Chem 1998;273:14424–9.
27. Rossig L, Badorff C, Holzmann Y, Zeiher AM, Dimmeler S. Glycogen synthase kinase-3 couples AKT-dependent signaling to the regulation of p21Cip1 degradation. J Biol Chem 2002;277:9684–9.
28. Koch A, Denkhaus D, Albrecht S, Leuschner I, von Schweinitz D, Pietsch T. Childhood hepatoblastomas frequently carry a mutated degradation targeting box of the beta-catenin gene. Cancer Res 1999;59:269–73.
29. Koch A, Waha A, Hartmann W, et al. Elevated expression of Wnt antagonists is a common event in hepatoblastomas. Clin Cancer Res 2005;11:4295–304.
30. Behrens J. Control of β-catenin signaling in tumor development. Ann N Y Acad Sci 2000;910:21–33; discussion 33–25.
31. Datta SR, Dudek H, Tao X, et al. Akt phosphorylation of BAD couples survival signals to the cell-intrinsic death machinery. Cell 1997;91:231–41.
32. Maurer U, Charvet C, Wagman AS, Dejardin E, Green DR. Glycogen synthase kinase-3 regulates mitochondrial outer membrane permeabilization and apoptosis by destabilization of MCL-1. Mol Cell 2006;21:749–60.
33. Opel D, Westhoff MA, Bender A, Braun V, Debatin KM, Fulda S. Phosphatidylinositol 3-kinase inhibition broadly sensitizes glioblastoma cells to death receptor- and drug-induced apoptosis. Cancer Res 2008;68:6271–80.